Computational fluid dynamic modeling of Nickel/Metal Hydride (Ni/MH) Battery during Charge Cycle

NABI JAHANTIGH, EBRAHIM AFSHARI
Department of Mechanical Engineering
Zabol University
Zabol, Zabol University
IRAN
njahantigh@zou.ac.ir

Abstract: - A three-dimensional mathematical model containing temporal and spatial coordinates with variable heat generation rates and temperature gradients across the battery is presented for analyzing the thermal behavior and obtaining the internal temperature profile of cylindrical Ni/MH battery. This model is performed to investigate the effects of thermal environment on battery electrochemical and thermal behaviors under various charging conditions. The governing equations are discretized using a finite volume based finite difference method and solved using a computational fluid dynamic code. Results shown that under the forced convection, the increase of the heat transfer coefficient can decrease the battery temperature, however, lead seriously to the less uniform temperature profile across the battery. The cell temperature rise is significant when the cell is charged at high rates and under poor cooling conditions, primarily due to the oxygen reactions occurring near the end of full charge. Overcharge can result in an increasingly higher temperature rise and a steeper temperature gradient within a battery.

1 Introduction

There has been an increasing interest in the potential use of nickel metal hydride (Ni/MH) battery power sources for many applications, such as in small electrical devices, power tools, and hybrid electric vehicles, due to their advantageous characteristics, which include high energy density, high rate capability, tolerance to overcharge and over-discharge, the lack of any poisonous heavy metals, and no electrolyte consumption during the charge/discharge cycle. The spirally wound design is generally employed in the manufacture of cylindrical Ni/MH battery. This design is of importance to battery in the improvement of the energy and power densities because of its lesser accessories when compared with the prismatic design [1]. However, the specific area is smaller for the spiral design, and the cylindrical batteries retain more heat and less uninformed temperature profiles under the larger loads. So it is important to study heat transport in these type batteries. Also In many applications, it is desirable to increase the size and capacity of rechargeable batteries. As the battery size increases, over potential heat and side reaction heat tend to accumulate. This makes the battery
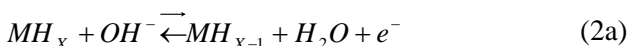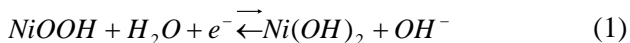
vulnerable to a large temperature distribution inside the battery, which in turn may cause a local battery overcharge in the high-temperature region. Therefore to improve a Ni/MH battery's charge performance and enlarge it, a precise understanding of the thermal behavior is required. Because of the highly reactive environment and compact nature of battery, it is hard to conduct calorimetric measurements to obtain the thermal data within a battery. This information is usually sought through modeling or simulation. Recent works are directed towards better understanding of the battery operation and performance Gu and Wang [2] presented a thermal-electrochemical coupled modeling approach to simultaneously predict battery electrochemical and thermal behaviors. Harmel et al [3] two different experimental methods presented to study the establishing of the heat balance. They also described the simulation of the temperature distribution by using finite element methods. Araki et al. [4] reported examines numerically and experimentally the thermal behavior of the Ni/MH cell during rapid charge and discharge cycles by a one dimentional model. Wu et al. [5] developed a two-dimensional and non-isothermal model for a Ni/MH cell that was

constructed on the planar electrode approximation. For simplicity, they are using a quasi-one-dimensional model to describe the battery behavior and performance characteristics. Yang and Liaw [6] escribed a recent progress in incorporating both oxygen and hydrogen recombinant cycles in a computational fluid dynamics based numerical model to simulate nickel metal hydride traction battery performance. Pan et al. [7] reported using CFD techniques similar to model isothermal charge and discharge behavior of Ni/MH cells. The model and experiments reported were focused on a commercial system and therefore only considered the oxygen recombinant cycle in the model. Verbrugge and Conell [8] constructed a traction battery model using an equivalent circuit model consisting of a parallel resistance-capacitance circuit in series with an ohmic resistance and a Ni/MH cell to allow simulation of the time-dependent voltage and thermal behavior over a range of relatively low current magnitudes. Ghassemi and Afshari [9, 10] have studied source term and effect of temperature distribution on Ni/Cd and Ni/MH batteries characteristic.

In this work, a three-dimensional mathematical model containing temporal and spatial coordinates, with variable heat generation rates and temperature gradients across the battery, was presented for analyzing the thermal behavior and obtaining the internal temperature profile of cylindrical Ni/MH battery to investigate the effects of thermal environment on battery electrochemical and thermal behaviors with different operational conditionsfuel cell

2 Model Description

Figure 1 shows a schematic drawing of a cylindrical Ni/MH battery. The cylindrical Ni/MH battery is composed of a porous positive electrode, a separate-or, and a negative electrode, which were spirally wound and inserted into a stainless steel case. This battery has the active material of NiOOH at the positive electrode and the active material of hydro-gen as a metal hydride at the negative electrode, with OH^- transferring between the two electrodes as a charge or discharge reaction proceeds. The charge/discharge reactions at the positive and negative electrodes are represented by Reactions 1 and 2a, respectively.

$$NiOOH + H_2O + e^- \overset{\rightarrow}{\leftarrow} Ni(OH)_2 + OH^- \qquad (1)$$

$$MH_X + OH^- \overset{\rightarrow}{\leftarrow} MH_{X-1} + H_2O + e^- \qquad (2a)$$

The negative electrode reaction (2a) can be divided into the following two equations: the hydrogen adsorption and desorption reaction (2b) and the water producing reaction (2c)

$$MH_X \overset{\rightarrow}{\leftarrow} MH_{X-1} + 1/2H_2 \qquad (2b)$$

$$1/2H_2 + OH^- \overset{\rightarrow}{\leftarrow} H_2O + e^- \qquad (2c)$$
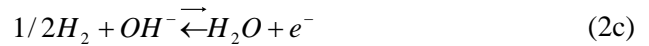
Because this battery uses an aqueous solution of KOH as electrolyte, OH^- is electrolyzed at the positive electrode when the charging voltage increases at the end of charge. This electrolyzing reaction produces O_2, which diffuses to the negative electrode, and reacts with water to regenerate OH^-. These are called side reactions. They are described (3) as a side reaction at the positive electrode, and (4a) as a side reaction at the negative electrode.

$$OH^- \overset{\rightarrow}{\leftarrow} 1/4O_2 + 1/2H_2O + e^- \qquad (3)$$

$$1/4O_2 + 1/2H_2O + e^- \overset{\rightarrow}{\leftarrow} OH^- \qquad (4a)$$
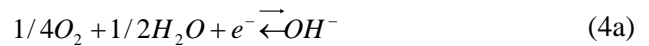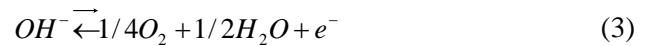
The side reaction (4a) at the negative electrode can be divided into the $H_2 - O_2$ reaction (4b) and the counteraction of (4c) for Reaction 2c.

$$1/2H_2 + 1/4O_2 + \rightarrow 1/2H_2O \qquad (4b)$$

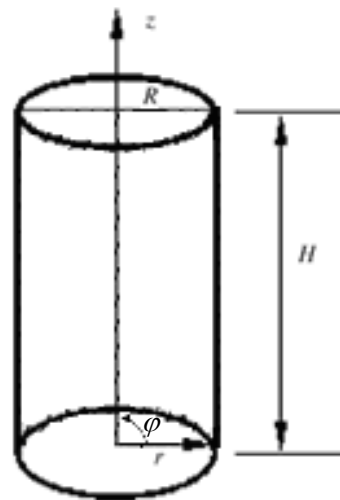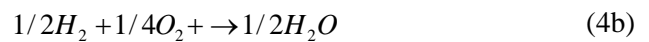$$H_2O + e^- \rightarrow 1/2H_2 + OH^- \qquad (4c)$$

Fig 1. schematic diagram of a cylindrical Ni/MH battery.

For a battery system, a general differential equation of thermal energy balance has been deduced based on first principles. With the assumptions of negligible heat effects due to viscous dissipation and pressure work, negligible convection term, no body

force, and no homogeneous chemical reactions, this general energy equation is reduced to

$$\frac{\partial(\rho c_p T)}{\partial t} = \nabla.(k\nabla T) + q \qquad (5)$$

Thermal modeling of a battery depends on source term behavior. The source term is a function of battery temperature and charging and discharging trend. To model the energy equation, this study incorporates the method introduced by Newman and Pals [10]. Source term for battery based on first law of thermodynamics is:

$$q = \sum_j I_j (U_j - T\frac{\partial U_j}{\partial T}) - IV + enthalpy\ of\ mixing\ term \qquad (8)$$
$$+\ phase\ change\ term$$

Where first term on the right hand side is enthalpy of reaction, second term is electrical work, third term is enthalpy of mixing and last term is phase change term. Neglecting third and fourth term of equation 8 [2] reduce to:

$$q = \frac{i}{L}(U - V - T\frac{\partial U}{\partial T}) \qquad (9)$$

Where open circuit potential of electrode reaction j (U_j) is linear function of temperature as follows:

$$U_j = U_{j,ref} + (T - T_{ref})\frac{\partial U_j}{\partial T} \qquad (10)$$

2.1 Initial and boundary conditions

The radiation conduction from the battery to the ambient is neglected and only cooling by convection is significant at the boundary. So the boundary and initial conditions can be written as follows.
Initial Conditions

$$T(r, \varphi, z) = 276K \qquad at: t = 0 \qquad (11)$$

Boundary conditions in r - direction

$$\frac{\partial T}{\partial r} = 0 \qquad at: r = 0 \qquad (12a)$$

$$-k_r\frac{\partial T}{\partial r} = h(T - T_\infty) \qquad at: r = R \qquad (12b)$$

Boundary conditions in φ – direction

$$T(r, \varphi, z) = T(r, \varphi + 2\pi, z) \qquad (13a)$$

$$\frac{\partial T(r, \varphi, z)}{\partial \varphi} = \frac{\partial T(r, \varphi + 2\pi, z)}{\partial \varphi} \qquad (13b)$$

Boundary conditions in z - direction

$$-k_z\frac{\partial T}{\partial z} = h(T - T_\infty) \qquad at: z = 0 \qquad (14a)$$

$$-k_z\frac{\partial T}{\partial z} = h(T - T_\infty) \qquad at: z = L \qquad (14b)$$

2.2 Numerical procedure

The governing equation, Eq 5, is discretized using a finite volume based on explicit method in finite difference method and is solved using a computational fluid dynamic code. The energy equation appears as a second order in space and first in time when discritized. To analysis the energy equation, the program uses an explicit based method to calculate temperature and other requirement, by 1/3 compare to implicit method. The selected time step, 0.0001 seconds, satisfies the stability criterion. To solve the energy equation, we fist solve the source term equation (9). Then the calculated rate of generation is updated in the energy equation and the temperature distribution is obtained. This will be repeated until the program converges. In addition, parameters for numerical calculation is selected in a form that comparison between numerical and experimental results are possible. Table 1 shows the values of parameters that are used in the numerical calculation

Table 1. Values of parameters used in the thermal modeling of a Ni/MH battery

Symbol	Unit	Value
H	cm	8.8
R	cm	3.3
ρ_e	g/cm^3	1.25
ρ_{Ni}	g/cm^3	3.55
ρ_{MH}	g/cm^3	7.49
ρ_{sep}	g/cm^3	0.9
$c_{p,e}$	$j/g\ K$	3.2
$c_{p,Ni}$	$j/g\ K$	0.88
$c_{p,MH}$	$j/g\ K$	0.35
$c_{p,sep}$	$j/g\ K$	1.9
t_{Ni}	cm	0.039
t_{MH}	cm	0.0127
t_{sep}	cm	0.089
$(dU/dT)_{ref}$	mV/K	-1.125

$(dU/dT)_{Ni}$	mV/K	-1.35
$(dU/dT)_{MH}$	mV/K	-0.836
$(dU/dT)_{sep}$	mV/K	-1.68
h	$w/m^2 k$	8 , 25

Numerical results

For verification purpose, the calculated surface temperature of Ni/MH battery is compared with the experimental data and is shown by Figure 2. As shown, both experimental and theoretical temperature data of Ni/MH battery are very close and show the same trend.
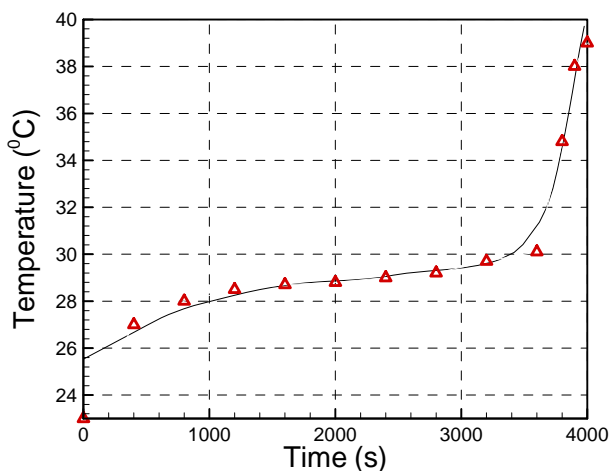

Fig 2. Comparison between experimental and numerical result of Ni/MH battery

Figure 3 plots the current density applied to the cell during charging at a voltage of 1.5 V. during battery charge current density decreases slowly, but during overcharge it increases, because the source term in the equation (5) during overcharge increasing rapidly.
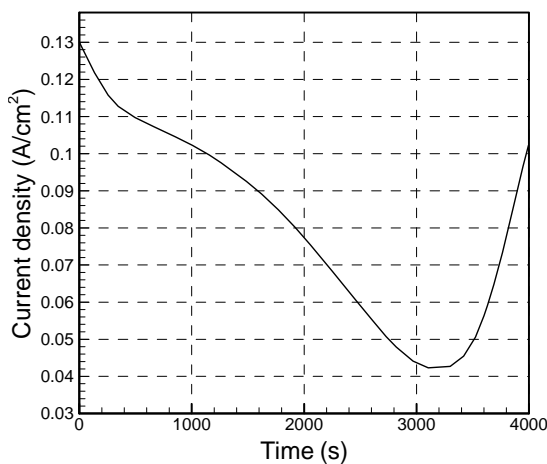

Figure 3. Current density applied to the cell during charging at a voltage of 1.5 V.

Figure 4 shows electrochemical and thermal behaviors of the Ni-MH cell during 1C charging. As the time increases, the cell potential increases more slowly and the potential peak becomes more pronounced. The cell temperature increases with time, indicating that the cell is exothermic when charged at 1C.
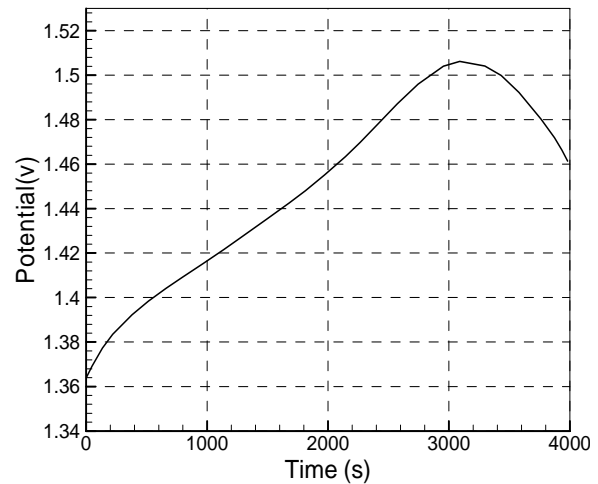

Fig 4. potential curves during 1C charging

Based on the results obtained from model calculation, the average surface temperature profile was shown in Figuer 5 at varying charging times under the natural convection $(h = 8W/m^2 K)$. The steeper parts of curve mean overcharge. The average surface temperature rises from $24^0 C$ to $30.2^0 C$ at the end of charge, when the imputed charge equals 110% of nominal capacity, the average surface temperature rises rapidly to $38.3^0 C$ overcharge.
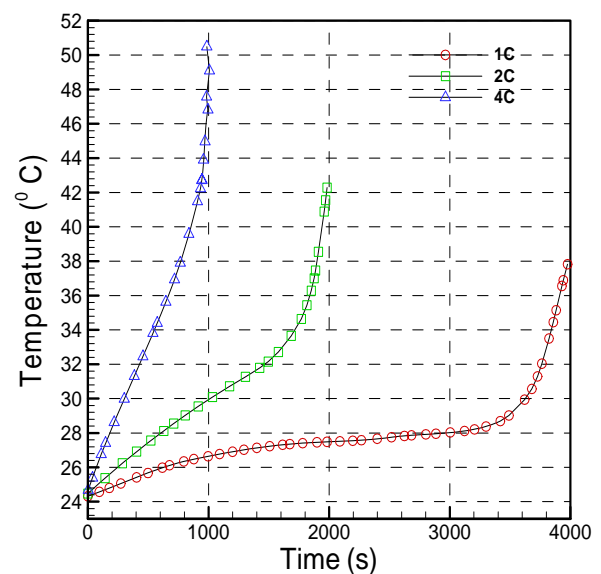

Fig 5. The average surface temperature variations of the battery during charge at 1C, 2C and 4C constant current

It is showed that the average surface temperature increases when the charging rates increase. The battery temperature increases with time, indicating that the battery is exothermic during charge. The results from the simulation are well in agreement with experimental measurements. In addition, it can be seen that under low charge rate, the temperature in the battery presents a small increase, however, under high charge rates; the temperature rise in the battery is very high.

Also Figure 6 compares the predicted temperature distributions in the surface of the battery under free and forced convection conditions. It is indicated that the battery temperature is remarkably lower under forced convection than free convection. This discrepancy is ascribed to the fact that forced convection can sufficiently dissipate the generated heat. The calculated results indicate increasing heat transfer coefficient can decrease the temperature of the battery. A lower temperature can be obtained at a higher heat dissipation rate.
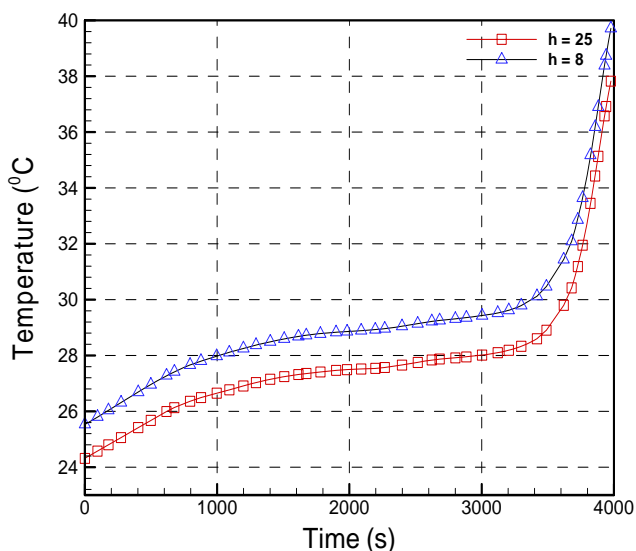

Fig 6. The average surface temperature variations with different heat-transfer coefficients

Figure 5 depicts the effect of charge input on temperature of Nickel/Metal Hydride battery battery. As shown, temperature increases at all charge input whish indicate an exothermic. The temperature increases slowly to about $30^0\,C$ up to 90% charge input. However, there is a sudden jump in temperature after 90% charge input, as shown by figure. At 120% charge input the temperature reaches a value of about $46^0\,C$. This is due to rate of change of generation inside the battery.
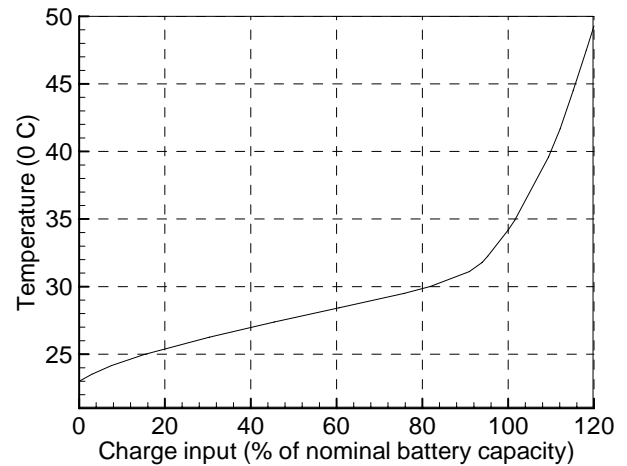

Fig 6. The average surface temperature variations with different heat-transfer coefficients

4 Conclusion

A general thermal energy equation has been derived using the finite volume technique, along with a local heat generation rate resulting from electrochemical reactions, phase transformation, and Joule heating. The model is multidimensional and capable of predicting the temperature distribution inside a cell in addition to the average cell temperature, thus providing a cost-effective tool to accurately predict the cell electrochemical and thermal behaviors, and most important, to identify the mechanisms responsible for thermal runaway.

Numerical simulations were performed to illustrate the significance of thermal and electrochemical coupling. The electrochemical and thermal behaveors of a Nickel/Metal Hydride battery were then explored numerically. Various operation modes and thermal conditions were examined. The cell temperature rise is significant when the cell is charged at high rates and under poor cooling conditions, primarily due to the oxygen reactions occurring near the end of full charge. The cell thermal behavior during constant-current charging was found to differ significantly from that during float charging.

Nomenclature

c_p	specific heat $(J\,kg^{-1}\,K^{-1})$
dU/dT	temperature coefficient $(mV\,K^{-1})$
h	Convective coefficient $(W\,cm^{-2}\,K^{-1})$
I	Current density $(A.cm^{-2})$

k	thermal conductivity $(W\,cm^{-1}\,K^{-1})$	
L	*battery length* (cm)	
q	heat generation rate $(J\,cm^{-3}\,s^{-1})$	
R	*battery radius* (cm)	
r	radial coordinate	
T	temperature (K)	
t	Thickness (cm)	
t	time (s)	
U	circuit cell potential-open (V)	
u	velocity vector $(cm\,s^{-1})$	

V	applied voltage (V)
z	horizontal coordinate
Greek symbols	
φ	peripheral coordinate
ρ	density $_{(g\,cm^{-3})}$
Subscript	
e	*Electrolyte*
MH	*MH electrode*
Ni	*Ni electrode*
ref	reference
sep	*polyamide separator*

References:

[1] J. Shi., F. Wu., Sh. Chen., and C. Zhang, Thermal analysis of rapid charging nickel/metal hydride batteries, *Journal of Power Sources*, Vol.157, 2006, pp. 592–599.

[2] W. B. Gu, and C. Y. Wang, Thermal-Electrochemical Modeling of Battery Systems, *Journal of Electrochemical Society*, Vol. 147, No.8, 2000, pp.2910-2922.

[3] J. Harmel, D. Ohmsb, U. Guth and K. Wiesener, Investigation of the heat balance of bipolar NiMH-batteries, *Journal of Power Sources*, Vol.155, 2006, pp.88–93.

[4] T. Araki, M. Nakayama, K. Fukuda, and K Onda, Thermal Behavior of Small Ni/MH Battery during Rapid Charge and Discharge Cycles, *Journal of Electrochemical Society*, Vol.152, No.6, 2005, pp.A1128-A1135.

[5] B. Wu, M. Mohammed, D.Brigham, R. Elder, R.E. White, A non–isothermal model of a nickel/methal hydride cell, *Journal of Power Sources,* Vol.101, 2001, pp.149–157.

[6] X. G. Yang and B. Y. Liaw, Numerical Simulation on Fast Charging Ni/MH Traction Batteries, *Journal of Electrochemical Society*, Vol.151, No2, 2004, pp. A265-A272.

[7] Y. H. Pan, V. Srinivasan, and C. Y. Wang, Journal of Power Sources, Vol.112, 2002, pp.298-???.

[8] M. W. Verbrugge and R. S. Conell, *Journal of Electrochemical Society,* Vol.149, 2002, pp.A45-A54

[9] [13] M. Ghassemi and E. Afshari, Thermal Analysis of Ni/Cd Batteries, 2nd International IIAA conference, 2003, pp. 150-156.

[10] [14] M. Ghassemi and E. Afshari, Effect of Temperature Variation on Nickel Cadmium and Nickel Metal Hydride Battery Parameters, ASME Heat Transfer/Fluids Engineering Summer Conference, 2004.